

**Three-jet cross section in hadron collisions at next-to-leading
order:
pure gluon processes**

Zoltán Trócsányi*

Department of Theoretical Physics, KLTE, Debrecen, Hungary

Abstract

The next-to-leading order three-jet cross section in hadron collisions is calculated in the simplified case when the matrix elements of all QCD subprocesses are approximated by the pure gluon matrix element. The longitudinally-invariant k_{\perp} jet-clustering algorithm is used. The important property of reduced renormalization and factorization scale dependence of the next-to-leading order physical cross section as compared to the Born cross section is demonstrated.

PACS numbers: 13.87Ce, 12.38Bx. Keywords: jets, QCD

*Zoltán Magyary fellow

The structure of hadronic final states in high energy collisions may be described in terms of jet characteristics. Nowadays, jet cross section data are used both for precise quantitative tests of QCD — such as measurement of the strong coupling α_s and QCD scale $\Lambda_{\overline{\text{MS}}}$ — and looking for signs of new physics beyond the standard model. Both of these objectives have been studied extensively in e^+e^- annihilation [1] that is characterized by a fixed high energy scale, namely the machine energy. One would also like to analyze the data of scattering processes at the highest available energy scale, where the signs of new physics is expected to be the most profound. The highest scale is in general found in hadron collisions. Unfortunately, there are important ambiguities which limit our ability to perform high precision quantitative studies with the jet cross sections observed in hadron collisions. In experiments ambiguities arise from the question of how to define a jet and from the systematic uncertainties of jet energy measurements. On the theoretical side, apart from the ubiquitous and ever decreasing uncertainty in the parton density functions [2], there still remains uncertainty in the choice of renormalization and factorization scales, the magnitude of the higher order corrections and the question of how to match the theoretical and experimental jet definitions. The theoretical ambiguity coming from these points can be decreased if the next-to-leading order corrections are calculated.

The most easily calculated next-to-leading order corrections to cross sections in hadron collisions are those to the inclusive one-jet and two-jet cross sections which have been available for some time [3,4]. These results have already proven to be extremely important: the significant enhancement in the experimental one-jet cross section over the result of the theory in the range $p_T^{\text{jet}} > 200 \text{ GeV}$ may be interpreted as signal of physics beyond the Standard Model [5].

In order to be able to calculate next-to-leading order corrections for more complex final states than the ones mentioned above — such as the three-jet cross section in hadron collisions —, two obstacles had to be overcome. Firstly, there was the issue of loop matrix elements which only recently have become available for all five-parton processes [6–8] necessary for a three-jet analysis. Secondly, the algorithm for the cancelation of infrared

divergences applied in ref. [4] were not directly applicable in processes with more complex final state kinematics. Recently, a number of general schemes have been proposed for achieving the cancelation of final state infrared singularities and mass factorization both in the framework of “phase space slicing” method [9] and “subtraction” method [10–12].

In this letter we present a brief summary of an analysis of three-jet cross sections using the algorithm of ref. [12], but in the simplified case when all squared matrix elements are approximated with that of the pure gluon subprocess. Thus the results shown are intended only for demonstrating the applicability of the subtraction scheme of ref. [12] in the case of hadron collisions rather than a serious theoretical description of the data. We anticipate however, similar conclusions as those drawn here will hold once the complete analysis with quarks included is finished.

According to the factorization theorem, the next-to-leading order infrared safe physical cross section at order $\alpha_s^{(N+1)}$ is a sum of two integrals,

$$\sigma = \mathcal{I}[2 \rightarrow N] + \mathcal{I}[2 \rightarrow N + 1], \quad (1)$$

where in the case of the pure gluon approximation for the squared matrix element, these integrals have the form

$$\begin{aligned} \mathcal{I}[2 \rightarrow n] = & \int dx_A f_{\text{eff}}(g, x_A) \int dx_B f_{\text{eff}}(g, x_B) \\ & \times \frac{1}{2x_A x_B s} \frac{1}{n!} \int d\Gamma^{(n)}(p_1^\mu, \dots, p_n^\mu) \langle |\mathcal{M}(g + g \rightarrow ng)|^2 \rangle \mathcal{S}_n(p_1^\mu, \dots, p_n^\mu). \end{aligned} \quad (2)$$

In this equation $d\Gamma^{(n)}$ is the usual n -particle phase space measure. There are two possibilities for the choice of the effective gluon densities. One can either imagine colliding glueballs [3], use a reference gluon density at a fixed μ_0 scale and evolve it to other scales with $N_f = 0$, or alternatively, one can use the effective gluon density [13],

$$f_{\text{eff}}(g, x) = f(g, x) + \frac{4}{9} \sum_q [f(q, x) + f(\bar{q}, x)]. \quad (3)$$

Our choice will be the latter one. There is still the question of what sort of strong coupling $\alpha_s(\mu)$ one should use in the pure gluon $\langle |\mathcal{M}(g + g \rightarrow ng)|^2 \rangle$ squared matrix elements.

We use the two-loop formula for the strong coupling with $N_f = 0$ and the QCD scale parameter in the modified minimal subtraction scheme, $\Lambda_{\overline{\text{MS}}}$ chosen to be 1600 MeV so as $\alpha_s(50 \text{ GeV}) \simeq 0.13$ is consistent with the value of $\alpha_s(50 \text{ GeV})$ observed in the real world with quarks. In this way we ensure that the relative size of the next-to-leading order correction is similar to that in the full QCD case. Note however, when we compare the order $\alpha_s^{(N+1)}$ cross section to the results of the Born-level calculation, we compute the Born cross section using the one-loop formula for α_s with the $\Lambda_{\overline{\text{MS}}} = 1100 \text{ MeV}$, which makes $\alpha_s(50 \text{ GeV})$ about 15% and the Born-level three-jet cross section about 50% bigger.

The function S_n in eq. (2) represents the physical quantity to be calculated. Among the numerous infrared safe physical quantities one can calculate with the technique presented ref. [12], an explicit example, that we use in the present analysis, is the next-to-leading order three-jet cross section in hadron collisions defined using the longitudinally-invariant k_\perp jet-clustering algorithm [14]. For hadron collisions the jet-clustering algorithm is a two-stage process, each characterized by a scale. The first step is the pre-clustering of hadrons into hard final state jets and beam jets. One sets the hardness scale of the jets to d_{cut} . Then for every final state hadron h_k and for every pair h_k, h_l one computes the corresponding value of the resolution variables d_{kB} and d_{kl} . There are several possibilities for the definition of the resolution variables. For instance, we may choose

$$d_{kB}^2 = p_k^2, \quad d_{kl}^2 = \min(p_k^2, p_l^2) R_{kl}^2, \quad (4)$$

where R_{kl} is the distance in (y, ϕ) -space,

$$R_{kl} = \sqrt{(\eta_k - \eta_l)^2 + (\phi_k - \phi_l)^2} \quad (5)$$

and (p_k, θ_k, ϕ_k) are the cylindrical coordinates of the three-momentum of hadron h_k with respect to the beam axis, with $\eta_k = -\ln \tan(\theta_k/2)$ being the corresponding pseudorapidity. (For other possibilities see ref. [14]). Having calculated the resolution variables, one considers the smallest value among $\{d_{kB}, d_{kl}\}$. If d_{ij} is the smallest value and $d_{ij} < d_{\text{cut}}$, then h_i and h_j are combined into a single cluster with momentum $p_{(ij)}^\mu$ according to a recombination

prescription and the algorithm starts again with hadrons h_i and h_j deleted from the final state and the ‘pseudoparticle’ of momentum $p_{(ij)}^\mu$ added to the final state. If d_{iB} is the smallest value and $d_{iB} < d_{\text{cut}}$, then hadron h_i is deleted from the final state and is included in the beam jets and the algorithm starts again. The algorithm stops if the smallest value is larger than the hardness scale d_{cut} . At the end of the algorithm one has two beam jets and several hard final state jets. The second step of the algorithm is the resolution of the event structure into sub-jets. For this step one defines a resolution parameter y_{cut} , $y_{\text{cut}} = Q_0^2/d_{\text{cut}}^2 \leq 1$. Using this resolution parameter and the set of final state hadron momenta pre-clustered into the hard final state jets one performs a k_\perp jet-clustering algorithm already familiar from studies in e^+e^- annihilation. For the sake of simplicity, here we choose $y_{\text{cut}} = 1$. With this choice we focus our attention to hard final state jets only, and suppress the second step of the clustering algorithm.

The principle of parton-hadron duality implies that we use the same clustering algorithm at parton level as defined at hadron level. Thus the measurement functions used for the next-to-leading order perturbative calculation of N hard final state jet production are

$$\mathcal{S}_{N+1}(p_1^\mu, \dots, p_{N+1}^\mu) = \Theta(d_{\min}^{(N+1)} > d_{\text{cut}}) + \Theta(d_{\min}^{(N+1)} < d_{\text{cut}})\Theta(d_{\min}^{(N+1 \rightarrow N)} > d_{\text{cut}}) \quad (6)$$

and

$$\mathcal{S}_N(p_1^\mu, \dots, p_N^\mu) = \Theta(d_{\min}^{(N)} > d_{\text{cut}}) \quad (7)$$

where

$$d_{\min}^{(n)} = \min(\{p_i^2, d_{ij}\} : i, j = 1, \dots, n, i \neq j), \quad (8)$$

and $d_{\min}^{(N+1 \rightarrow N)}$ is the minimal value of the resolution variables after one clustering step. In eq. (6) the first term represents the $N+1$ -jet production, while the second one represents the production of N jets and either a soft parton, or a hard parton collinear with the beam axis, thus included in the beam jets or N -jet production such that all final state partons are hard, but two of them are collinear, thus combined into a single jet. It is not difficult to check

that these measurement functions are infrared safe if any sensible recombination scheme [14] is applied. In our analysis, we use the p_t -weighted recombination. In this scheme the transverse momentum, pseudorapidity and azimuth of the pseudoparticle (ij) are defined as

$$p_{t(ij)} = p_{ti} + p_{tj}, \quad (9)$$

$$\eta_{t(ij)} = \frac{p_{ti}\eta_{ti} + p_{tj}\eta_{tj}}{p_{t(ij)}}, \quad (10)$$

$$\phi_{t(ij)} = \frac{p_{ti}\phi_{ti} + p_{tj}\phi_{tj}}{p_{t(ij)}}. \quad (11)$$

We remark that any other experimental cut, such as cut in the rapidity window, or a p_t trigger should also be included in the measurement functions. In our analysis, we required that for the rapidity of jets $|\eta| < 3$ and the sum of the transverse momenta of the observed particles $p_t^{\text{sum}} > 100$ GeV.

We now turn to the description of our results which were obtained at $\sqrt{s} = 1800$ GeV machine energy and using the HMRS(B) [15] parton distributions. In Fig. 1 we plot the total three-jet cross section both at Born level and at next-to-leading order for a fixed value of $d_{\text{cut}} = 70$ GeV vs μ which is the common renormalization and factorization scale. This plot demonstrates that over a wide range of μ values the theoretical uncertainty coming from the scale dependence is sizeably reduced in the next-to-leading order result as compared to the result of a Born calculation. In particular, one expects on general grounds that μ should be chosen of the order of the hard scale d_{cut} . If one varies μ in the range of $d_{\text{cut}}/2 < \mu < 2d_{\text{cut}}$, then the change in the next-to-leading order cross section is less than 1/6 of the change in the Born-level result. Thus the inclusion of the higher order correction decreases the uncertainty in the theoretical prediction by a factor of larger than 6. Similar conclusion can be drawn from plots at other d_{cut} values in the range of $20 \text{ GeV} < d_{\text{cut}} < 200 \text{ GeV}$. This can also be seen from Fig. 2, where the overall size of the three-jet cross section can be read off from a differential cross section $d_{\text{cut}}^3 d\sigma/dd_{\text{cut}}$ plotted vs d_{cut} . The wide gray band shows the result of a Born level calculation with μ varied between $d_{\text{cut}}/2 < \mu < 2d_{\text{cut}}$, while the narrower black band inside is the next-to-leading order result with the same scale variation.

In order to give the reader some feeling about the errors of the Monte Carlo integrations,

in Fig. 3 we plot the size of the Born-level cross section and the higher order correction to it together with the statistical errors of these results at $\mu = d_{\text{cut}}$. The statistical error of the Born result is below 1%, while the statistical error of the full next-to-leading order cross section plotted in Fig. 2 is below 10%.

In conclusion, we have calculated the three-jet cross section for the longitudinally invariant k_{\perp} jet-clustering algorithm in hadron collisions for the simplified case when the matrix elements of all subprocesses are approximated by those of the pure gluon subprocess. The motivation for the particular choice of the jet definition is simply the pleasant property of the clustering algorithm that it uniquely assigns all final state particles to a certain jet. Using this definition one avoids the problem of jet separation in case of overlapping jets that occurs when cone jet definition is used. We used the subtraction method of ref. [12] for canceling the infrared singularities. This method has the important feature that the physical quantity to be calculated is well separated from the theoretical problems of cancellation of infrared singularities and can easily be changed in a modular fashion in the Monte Carlo program. Thus the particular choice for the jet definition is by no means essential. We have found that the inclusion of the higher order correction improves dramatically our theoretical description of the three-jet cross section: the ambiguity coming from the arbitrary choice of the renormalization and factorization scales is reduced by a factor of at least six. Although the current analysis is not complete in the sense that we have not used the full QCD matrix elements, we anticipate similar conclusions once the effect of quarks is included.

This research was supported in part by the EEC Programme "Human Capital and Mobility", Network "Physics at High Energy Colliders", contract PECO ERBCIPDCT 94 0613 as well as by the Foundation for Hungarian Higher education and Research, the Hungarian National Science Foundation grant OTKA T-016613 and the Research Group in Physics of the Hungarian Academy of Sciences, Debrecen.

REFERENCES

- [1] See e.g., B. R. Webber, QCD and Jet Physics, Proceedings of the XXVII International Conference on High Energy Physics, ed.: P. J. Bussey and I. G. Knowles, IOP Publishing Ltd (1995); S. Bethke, Status of alpha-s measurements, Proceedings of the 30th Rencontres de Moriond: QCD and High Energy Hadronic Interactions, ed.: J. Tran Thanh Van (1995).
- [2] A. D. Martin, R. G. Roberts and W. J. Stirling, Phys. Rev. D **50**, 6734 (1994), Phys. Lett. **B354**, 155 (1995); CTEQ collaboration: J. Botts et al., Phys. Lett. **B304**, 159 (1993), H. L. Lai et al., Phys. Rev. D **51**, 4763 (1995).
- [3] S. D. Ellis, Z. Kunszt, D. Soper, Phys. Rev. Lett. **62**, 726 (1988).
- [4] S. D. Ellis, Z. Kunszt, D. Soper, Phys. Rev. Lett. **64**, 2121 (1990), Phys. Rev. Lett. **69**, 1496 (1992), Phys. Rev. D **40**, 2188 (1989); Z. Kunszt, D. Soper, Phys. Rev. D **46**, 192 (1992); F. Aversa, M. Greco, P. Chiappetta and J. Ph. Guillet, Phys. Rev. Lett. **65**, 401 (1990), Zeit. Phys. C **49**, 459 (1991).
- [5] CDF collaboration: F. Abe et al., preprint FERMILAB-PUB-96/020-E (1996).
- [6] Z. Bern L. Dixon, and D. A. Kosower, Phys. Rev. Lett. **70**, 2677 (1993).
- [7] Z. Kunszt, A. Signer and Z. Trócsányi, Phys. Lett. **B336**, 529 (1994).
- [8] Z. Bern L. Dixon, and D. A. Kosower, Nucl. Phys. **B437**, 259 (1995).
- [9] W. T. Giele and E. W. N Glover, Phys. Rev. D **46**, 1980 (1992); W. T. Giele, E. W. N Glover and D. A. Kosower, Nucl. Phys. **B403**, 633 (1993).
- [10] S. Frixione, Z. Kunszt, A. Signer, preprint ETH-TH/95-42.
- [11] S. Catani and M. H. Seymour, preprint CERN-TH/96-28.
- [12] Z. Nagy and Z. Trócsányi, preprint KLTE-DTP/96-1.
- [13] B. L. Combridge and C. J. Maxwell, Nucl. Phys. **B239**, 429 (1984); UA1 Collab., G. Arnison et al., Phys. Lett. **136B**, 294 (1984).
- [14] S. Catani, Yu. L. Dokshitzer, M. H. Seymour and B. R. Webber, Nucl. Phys. **B406**, 187 (1993); a similar algorithm, designed for defining inclusive cross sections, was suggested in S. D. Ellis and D. Soper, Phys. Rev. D **48**, 3160 (1993).
- [15] P. N. Harriman, A. D. Martin, R. G. Roberts and W. J. Stirling, Phys. Rev. D **42**, 798 (1990).

FIGURES

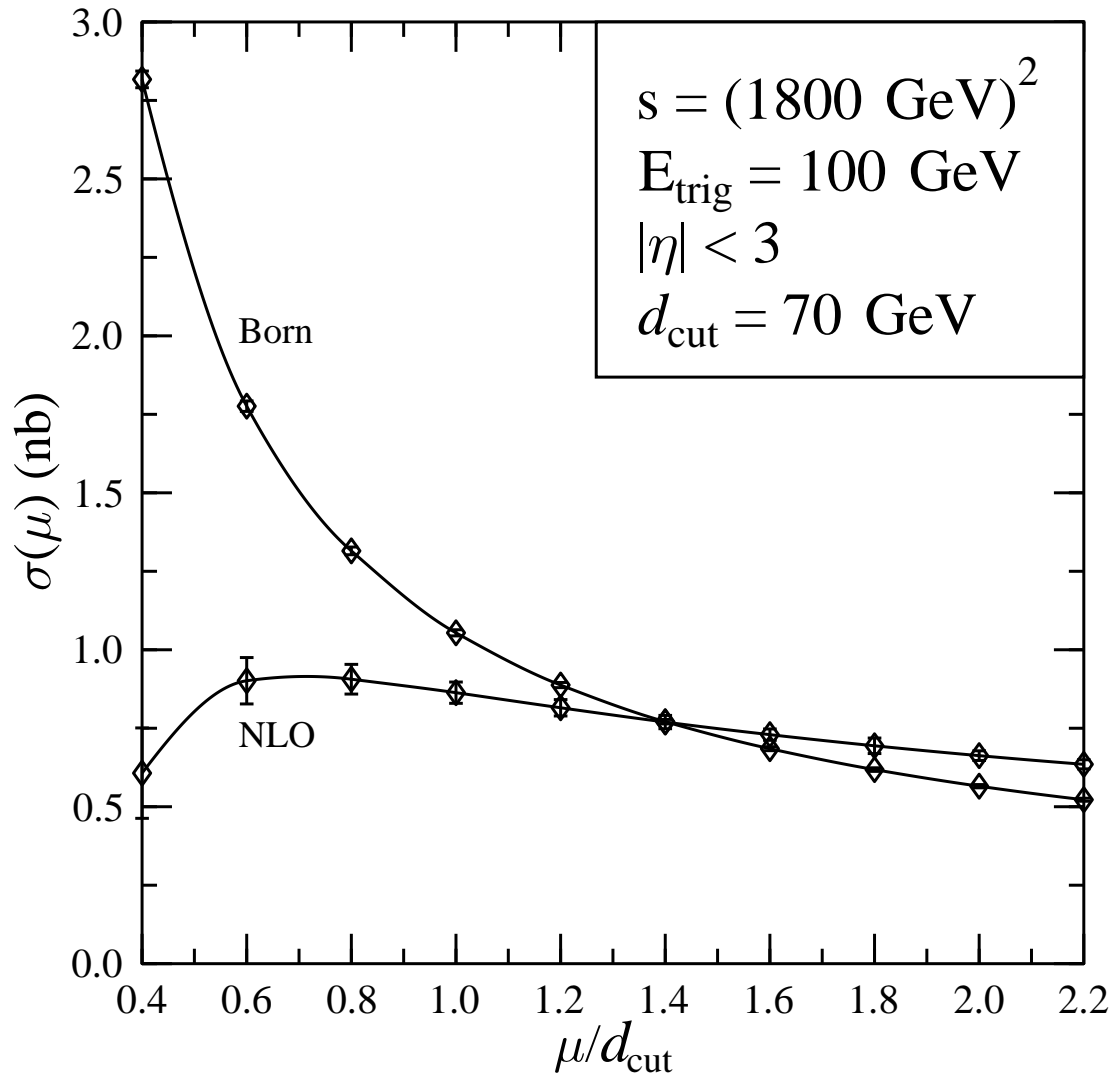


FIG. 1. Total three-jet cross section $\sigma(d_{\text{cut}} = 70 \text{ GeV})$ vs μ at the Born and α_s^4 level.

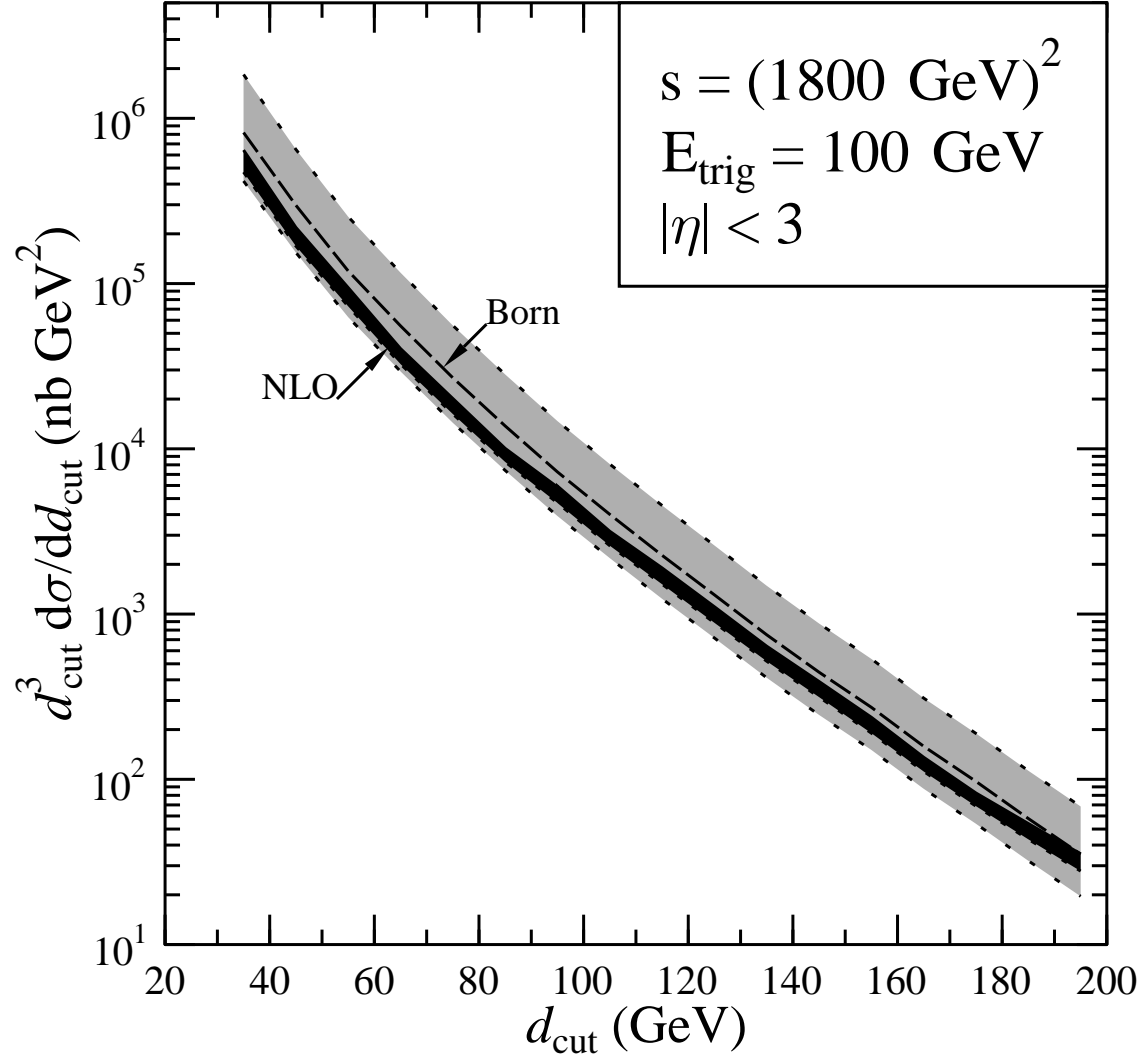


FIG. 2. Differential three-jet cross section $d_{\text{cut}}^3 d\sigma/dd_{\text{cut}}$ vs d_{cut} for $0.5d_{\text{cut}} < \mu < 2d_{\text{cut}}$ at Born level (gray band) and at next-to-leading order (black band).

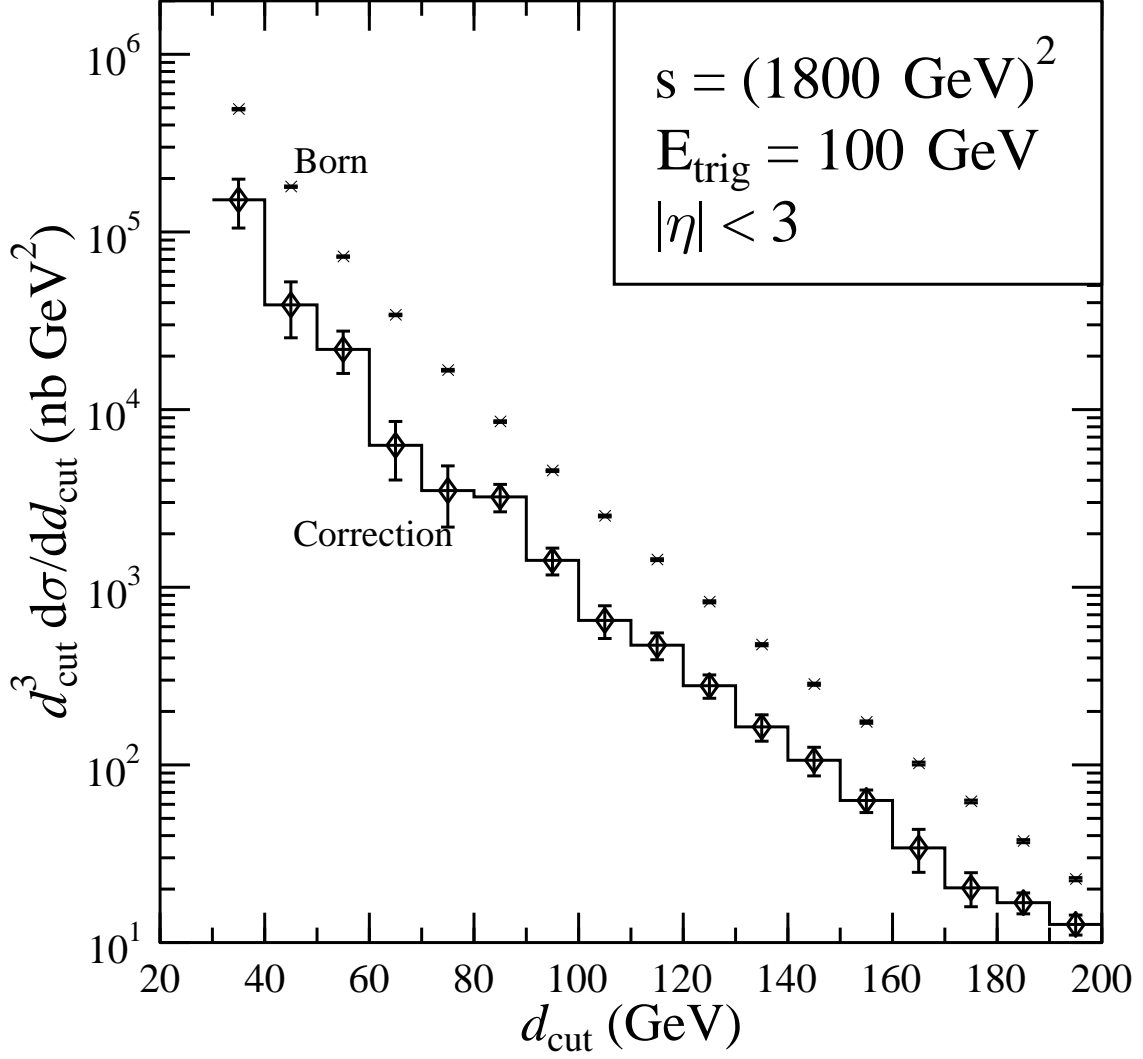


FIG. 3. Differential three-jet cross section $d^3_{\text{cut}} d\sigma/dd_{\text{cut}}$ vs d_{cut} for $\mu = d_{\text{cut}}$ at Born level (crosses) and the higher order correction to it (histogram). The errobars indicate the statistical error of the Monte Carlo integration.